

Comparative study of nudged elastic band and molecular dynamics methods for diffusion kinetics in solid-state electrolytes

Aming Lin(林啊鸣), Jing Shi(石晶), Su-Huai Wei(魏苏淮), and Yi-Yang Sun(孙宜阳)
Citation: Chin. Phys. B, 2024, 33 (**8**): 086601. DOI: 10.1088/1674-1056/ad5d9a

What follows is a list of articles you may be interested in

Hydrogen diffusion in C_1' phase clathrate hydrate

Zixuan Song(宋姿璇), Ziyue Zhou(周子岳), Yanwen Lin(林演文), Qiao Shi(石桥), Yongchao Hao(郝勇超),Yuequn Fu(付越群), Zhisen Zhang(张志森), and Jianyang Wu(吴建洋)
Chin. Phys. B, 2023, 32 (**6**): 066602. DOI: 10.1088/1674-1056/accd4b

Strain effects on Li^+ diffusion in solid electrolyte interphases: A molecular dynamics study

Xiang Ji(姬祥) and Junqian Zhang(张俊乾)
Chin. Phys. B, 2023, 32 (**6**): 066601. DOI: 10.1088/1674-1056/ac9606

Sintering reaction and microstructure of *M*Al (*M* = Ni, Fe, and Mg) nanoparticles through molecular dynamics simulation

Yuwen Zhang(张宇文), Yonghe Deng(邓永和), Qingfeng Zeng(曾庆丰), Dadong Wen(文大东), Heping Zhao(赵鹤平), Ming Gao(高明), Xiongying Dai(戴雄英), and Anru Wu(吴安如)$
Chin. Phys. B, 2020, 29 (**11**): 116601. DOI: 10.1088/1674-1056/aba2dd

Molecular dynamics simulation of thermal conductivity of silicone rubber

Wenxue Xu(徐文雪), Yanyan Wu(吴雁艳), Yuan Zhu(祝渊), Xin-Gang Liang(梁新刚)
Chin. Phys. B, 2020, 29 (**4**): 046601. DOI: 10.1088/1674-1056/ab7743

Collective diffusion in carbon nanotubes: Crossover between one dimension and three dimensions

Pei-Rong Chen(陈沛荣), Zhi-Cheng Xu(徐志成), Yu Gu(古宇), Wei-Rong Zhong(钟伟荣)
Chin. Phys. B, 2016, 25 (**8**): 086601. DOI: 10.1088/1674-1056/25/8/086601

RAPID COMMUNICATION

Comparative study of nudged elastic band and molecular dynamics methods for diffusion kinetics in solid-state electrolytes

Aming Lin(林啊鸣)[1,2], Jing Shi(石晶)[3], Su-Huai Wei(魏苏淮)[4,†], and Yi-Yang Sun(孙宜阳)[1,2,‡]

[1] *State Key Laboratory of High Performance Ceramics and Superfine Microstructure, Shanghai Institute of Ceramics, Chinese Academy of Sciences, Shanghai* 201899, *China*

[2] *Center of Materials Science and Optoelectronics Engineering, University of Chinese Academy of Sciences, Beijing* 100049, *China*

[3] *Department of Physics, Jiangxi Normal University, Nanchang* 330022, *China*

[4] *Eastern Institute of Technology, Ningbo* 315200, *China*

(Received 20 June 2024; revised manuscript received 20 June 2024; accepted manuscript online 2 July 2024)

Considerable efforts are being made to transition current lithium-ion and sodium-ion batteries towards the use of solid-state electrolytes. Computational methods, specifically nudged elastic band (NEB) and molecular dynamics (MD) methods, provide powerful tools for the design of solid-state electrolytes. The MD method is usually the choice for studying the materials involving complex multiple diffusion paths or having disordered structures. However, it relies on simulations at temperatures much higher than working temperature. This paper studies the reliability of the MD method using the system of Na diffusion in MgO as a benchmark. We carefully study the convergence behavior of the MD method and demonstrate that total effective simulation time of 12 ns can converge the calculated diffusion barrier to about 0.01 eV. The calculated diffusion barrier is 0.31 eV from both methods. The diffusion coefficients at room temperature are 4.3×10^{-9} cm^2·s^{-1} and 2.2×10^{-9} cm^2·s^{-1}, respectively, from the NEB and MD methods. Our results justify the reliability of the MD method, even though high temperature simulations have to be employed to overcome the limitation on simulation time.

Keywords: nudged elastic band method, molecular dynamics, solid electrolyte, ion transport, density functional theory

PACS: 66.30.J–, 71.15.Mb **DOI:** 10.1088/1674-1056/ad5d9a

1. Introduction

Lithium-ion batteries (LIBs) and sodium-ion batteries (NIBs) have garnered considerable attention as current and next-generation energy storage devices.[1–5] With an increasing emphasis on high safety and the adoption of metal anodes to enhance battery capacity, research on electrolytes has gradually shifted from traditional organic liquids to inorganic solids to realize all-solid-state batteries.[6,7] In this trend, the discovery of fast Li and Na ion conductors becomes crucial to serve as solid-state electrolytes.[8–12]

Despite commendable progress, a comprehensive understanding of ion transport mechanisms in fast ion conductors remains challenging.[13,14] Experimental evaluations of ionic conductivity often encounter issues due to uncertainties introduced by complex structures.[15,16] Factors such as defects, impurities, and irregularities in the preparation process contribute to such uncertainty.[17] Additionally, the rapid diffusion of ions, coupled with uncertain site occupancy in fast ion conductors, poses challenges in determining ion transport mechanisms through experimental methods.[12] To address these challenges, computational methods serve as powerful and complementary tools.[13,18–21]

Ion diffusion in solids occurs through hopping among the lattice and interstitial sites, which needs to overcome energy barriers. The nudged elastic band (NEB) and molecular dynamics (MD) methods are the most commonly used methods for studying the diffusion kinetics. In the NEB method, the direct output is the diffusion barrier, from which the diffusion coefficient at a given temperature can be estimated by calculating the attempt frequency. In contrast, the MD method directly gives the diffusion coefficient at different temperatures, from which the activation barrier can be obtained using the Arrhenius relation.

The NEB method is rooted in transition state theory and proves effective for calculating diffusion barriers.[22–24] It is particularly suited in scenarios where the atomic structures are ordered so that the transition path is well defined with the initial and final states uniquely specified. There also exist methods for handling multiple-barrier diffusion problems by the NEB method if all possible diffusion paths are known.[25] However, when studying diffusion in complex systems with multiple diffusing ions or high disorder, exemplified by $Li_5La_3Ta_2O_{12}$,[26,27] Li_3PS_4,[28] and Li_7PS_6,[19] the NEB method will expose its limitation in obtaining the statistical average of the diffusion barriers. For such systems, the MD method offers a more suited solution for studying the diffu-

†Corresponding author. E-mail: suhuaiwei@eitech.edu.cn

‡Corresponding author. E-mail: yysun@mail.sic.ac.cn

© 2024 Chinese Physical Society and IOP Publishing Ltd

sion kinetics.

MD simulations track ion movements at the atomic scale without predefined diffusion paths, allowing for the consideration of simultaneous diffusion of multiple ions, thereby better simulating ion diffusion in complex systems.[29–32] While the MD method provides detailed insights into ion diffusion, it is typically limited by the simulation time in sub-nanosecond regime. Therefore, only carrying out simulations at high temperatures can give rise to sufficient displacements of diffusing ions for acquiring the diffusion coefficients. Then, an extrapolation to low temperature has to be employed to predict the behavior at room temperature.[33,34] As the MD simulations could be subject to large uncertainties, whether the errors are amplified during the extrapolation necessitates a systematic comparison between the NEB and MD results.

In this study, we benchmark the NEB and MD methods by investigating Na diffusion in MgO. Selected for its simple rock salt structure with well-defined diffusion path between neighboring tetrahedral sites, MgO serves as an ideal host material. NEB calculations reveal a Na diffusion barrier of 0.31 eV in MgO. Enabled by machine-learning interatomic potentials, we systematically study the convergence behaviors of the MD method, which yields nearly the same diffusion barrier if the calculations are properly converged. We have paid particular attention to the convergence issue. The diffusion coefficient determined by the MD method at room temperature is also on the same order of magnitude as that obtained by the NEB method, reinforcing agreement between the two methods. This work furnishes a rigorous assessment of the MD method, and affirms the validity of a large body of data produced by this method.

2. Computational method

First-principles density functional theory (DFT) calculations were conducted using the Vienna *Ab Initio* Simulation Package (VASP).[35] Projector augmented wave (PAW) potentials described the interaction between ion cores and valence electrons.[36] The PAW potentials for Mg and O contain two and six valence electrons, respectively. The soft PAW potential for O supplied by the VASP package was used in this work. Plane-wave basis set with cutoff energy of 280 eV was sufficient to obtain converged results. The Perdew–Burke–Ernzerhof (PBE) form of the generalized gradient approximation served as the exchange–correlation functional.[37] Figure 1(a) depicts the supercell of MgO, consisting of 216 atoms. For this supercell, we used the Γ point to represent the Brillouin zone.

This work is mainly concerned with the ion diffusion properties. In general, a deliberate distinction should be made between diffusion barrier (E_b) and activation energy (E_a). As discussed above, E_b characterizes individual events with the initial and final structures well specified, while E_a describes a collective behavior or a statistical process. In the present case, the two quantities are supposed to be consistent as a result of the simple diffusion path for the benchmarking purpose.

The macroscopic diffusion coefficient (D) correlates with the microscopic ionic dynamics by[38]

$$D = \frac{1}{6} f Z d^2 \Gamma. \tag{1}$$

Here, f is the correlation factor, which equals 1 for diffusion of dilute interstitial atoms.[38,39] Z is the number of neighboring vacant sites, which is 6 for interstitial Na diffusion in MgO. d is the hopping distance, which is half of the lattice constant of MgO in this work. Γ is the hopping rate given by

$$\Gamma = \nu \exp\left(-\frac{E_b}{k_B T}\right), \tag{2}$$

where k_B is the Boltzmann constant and T is the absolute temperature. The prefactor ν denotes an attempt frequency. For a system containing N atoms, ν can be evaluated as[40]

$$\nu = \prod_{i=1}^{3N} \nu_i / \prod_{j=1}^{3N-1} \nu'_j. \tag{3}$$

Here, ν_i and ν'_j represent the real normal vibrational frequencies at the initial state and the transition state, respectively, and N is the total number of atoms in the system under study. Once the E_b is determined by the NEB method, the diffusion coefficient can be evaluated by the equations above.

Different from the NEB method, in the MD method the diffusion coefficient is obtained by utilizing the Arrhenius relation, while the activation energy E_a is a by-product of the fitting process. *NVT* simulations were conducted at temperatures of 1000 K, 1143 K, 1333 K, and 1600 K with the Nose–Hoover thermostat.[41] Two primary purposes of this work are (i) benchmarking the consistency of the NEB and MD methods in terms of calculated activation barrier and diffusion coefficient and (ii) the convergence issues revolving the MD method with respect to effective simulation time, defined as the product of the actual simulation time and the total number of diffusing ions. For the second purpose, we carried out 500 runs of MD simulations at each temperature to determine the E_a. Each MD run is 67.5 ps with a time step of 1.5 fs. In the MD method, the diffusion coefficient D at a given temperature was obtained by the mean square displacement (MSD) as a linear function of time interval t

$$\mathrm{MSD}(t) = 6Dt, \tag{4}$$

where the MSD at a given temperature is evaluated using the MD trajectory.[42] Once the D is obtained at the selected temperatures, the E_a can be determined through the Arrhenius relation

$$D(T) = D_0 \exp\left(-\frac{E_a}{k_B T}\right). \tag{5}$$

The D at the temperatures other than the selected ones for carrying out the MD simulations can be obtained by linear interpolation or extrapolation.

For enhanced computational efficiency, we incorporated machine-learning (ML) potentials into our MD simulations. This implementation followed an "on-the-fly" (or active learning) scheme, triggering DFT calculations as necessary.[43–46] The process commenced with DFT calculations for the initial structures. Total energies and atomic forces obtained from these DFT calculations were utilized to train the machine-learning force fields (ML-FF). Then, atomic forces predicted by ML-FF were applied to new structures. In cases when a new structure is beyond the description by the training set, DFT calculation is called again to update the ML-FF. The seamless alternation between DFT and ML-FF steps combines the accuracy of the former and the efficiency of the latter, resulting in a substantial reduction in computational time. It is this ML-FF method that enables the MD simulations conducted in this work, which together amount to 0.135 microseconds.

3. Results and discussion

For the purpose of benchmarking the MD method, we first need to choose a suitable material system. MgO in the rock salt structure with two fcc sublattices of anions and cations[47] is adopted here. In this structure, the octahedral sites are fully occupied, while the tetrahedral sites are unoccupied serving as interstitial sites. This inherent simplicity in structure provides a clear diffusion path, occurring between two vacant tetrahedra. We are interested in the diffusion of monovalent ions and considered all alkali metal elements. Employing the NEB method, we calculated the diffusion barriers of Li, Na, K, Rb and Cs ions in MgO. The results are shown in Fig. 1(b), where an interesting V-shape trend is observed. The E_b of 0.31 eV for Na is close to the common values reported in the literature on solid-state electrolytes, we will focus on the Na diffusion in this work. Figure 1(c) shows the diffusion path of Na with the atomic structures of initial, final and transition states shown as insets. The path is symmetric as the initial and final states are equivalent and the transition state is at the midway point. By calculating the vibrational frequencies of the initial and transition states, we obtained $\nu = 1.43$ THz from Eq. (3). Then, using Eqs. (1) and (2) we estimated the diffusion coefficient D at room temperature to be 4.3×10^{-9} cm^2·s^{-1} for Na interstitial diffusion in MgO.

There is an issue regarding whether the NEB calculations should be conducted at neutral or charged state, which is related to whether a Na atom or a Na ion is diffusing. To address this, we conducted an analysis of the electronic structure of the Na-doped MgO system. Figure 1(d) shows the band structure of the Na-doped supercell. As the neutral and charged calculations yield almost the same band structures, we only show the neutral case. The absence of defect levels in the band gap suggests that Na in MgO is a shallow donor. In such a case, even in neutral state calculations, the Na atom is already ionized and the charge state should not significantly affect the NEB calculations. We also carried out NEB calculations at the 1+ charge state. In these calculations, one electron was removed from the system, which was compensated by adding a uniform charge background to the supercell. As shown in Fig. 1(b), for all alkali metal elements, the calculated barriers show negligible difference between the charged and neutral states. In subsequent studies, we adopted the neutral state calculations.

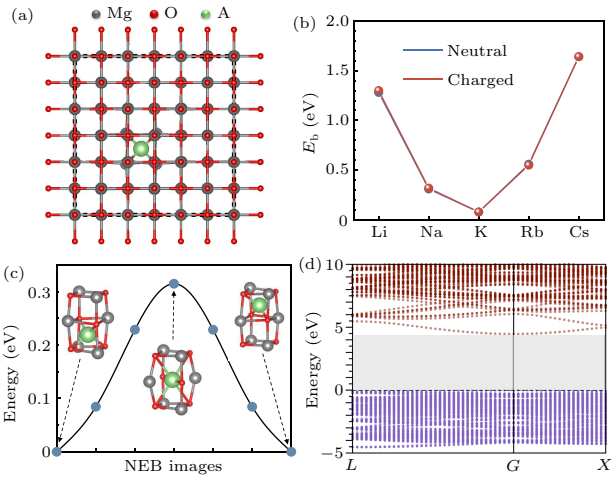


Fig. 1. (a) Supercell of MgO (marked by a dashed frame) with an inserted alkali metal ion A (A = Li, Na, K, Rb or Cs) at an interstitial site. (b) Calculated diffusion barrier (E_b) for the five alkali metal ions in both charged and neutral states using the NEB method. (c) Energy profile from the NEB method for Na diffusion in MgO. The insets show the local atomic structures of the initial, transition and final states. (d) Band structure of Na-doped MgO supercell in neutral charge state, showing the absence of defect states in the band gap (gray-colored region).

After obtaining E_b from the NEB calculations, we next evaluated the activation energy E_a using the MD method. Before that, to assess the reliability of the ML-FF, we carried out MD simulations at 1000 K, 1143 K, 1333 K and 1600 K based on the ML-FF. Each simulation was run for 45000 steps with time step of 1.5 fs. The initial 5000 steps were not used for statistical analyses. Then, over the subsequent 40000 steps we extracted 100 structures at a 400-step interval. For each structure, single-point DFT calculations were performed. Figure 2(a) displays the correlation of the total energies calculated from the DFT and ML-FF, which exhibits a good linear relationship with the root mean square error (RMSE) of 0.070 eV. Figure 2(b) displays the correlation of atomic forces acting on Na atoms. The RMSE for the forces is 0.079 eV·Å^{-1}. The comparisons above suggest that the ML-FF method can reliably describe the Na diffusion in the MgO lattice.

With the accuracy of the ML-FF method assessed, we proceeded to calculate the MSDs for Na diffusion in MgO.

We employed the same 216-atom MgO supercell as in NEB calculations. As mentioned earlier, at each temperature we carried out 500 MD runs of 45000 steps (67.5 ps). For each run, the initial velocities were randomly assigned. Figure 3(a) shows the MSD as a function of time interval t derived from randomly selected five MD runs at 1600 K. The following formula:[42]

$$\mathrm{MSD}(t) = \frac{1}{N_{\mathrm{step}}} \sum_{i=1}^{N_{\mathrm{step}}} |\boldsymbol{r}(t_i + t) - \boldsymbol{r}(t_i)|^2 \tag{6}$$

was used to calculate the MSD, where N_{step} is the number of MD steps used to evaluate MSD and $\boldsymbol{r}(t_i)$ is the coordinate of the Na ion at the time of the i-th step. It is seen that none of the individual MD runs yields a linear MSD. So the diffusion coefficient D cannot be reliably extracted. In contrast, if averaging over the 500 runs, as shown in Fig. 3(b), excellent linear relationship can be obtained at all temperatures.

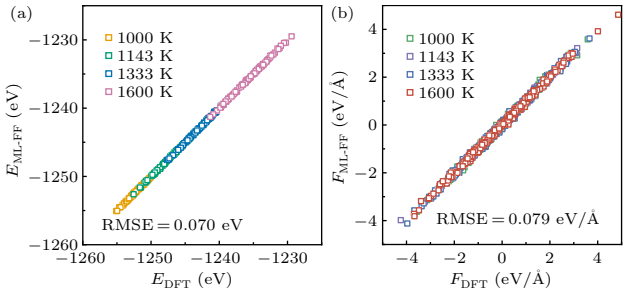


Fig. 2. Comparisons of total energies (a) and atomic forces (b) calculated for the Na-doped MgO system using density functional theory (DFT) and machine-learning force field (ML-FF). The comparisons were based on 400 snapshot structures from MD simulations at four temperatures (100 structures from each temperature).

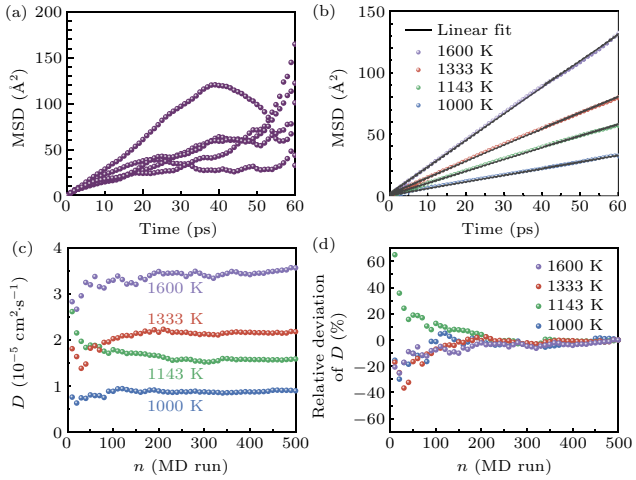


Fig. 3. (a) MSDs derived from five randomly selected 60-ps MD runs at 1600 K for a single Na ion diffusion in MgO. (b) Averaged MSD from 60-ps 500 MD runs at four temperatures. (c) Diffusion coefficient D as a function of the number of MD runs (n) used to average the MSD. (d) Relative deviation of D as a function of n, where the values derived using 500 MD runs were taken as the references.

To study the convergence of D with respect to the number of MD runs, we randomly selected n runs from the 500 runs at each temperature to calculate D. The calculated D as a function of n is shown in Fig. 3(c). By taking the D values averaged over 500 runs as the references, we plotted the relative deviations from the references in Fig. 3(d). It is seen that good convergence is achieved around 200 runs, which amount to an effective simulation time of 12 ns. This figure can serve as a guide line being useful in terms of order of magnitude, i.e., the total simulation time multiplying the number of diffusing ions needs to be on the order of 12 ns. Practical solid-state electrolyte materials are rich in diffusing ions (e.g., Li and Na) so that the simulation supercells contain multiple diffusing ions (denoted by N_{atom}). If considering that the diffusing ions are not correlated, the actual MD simulation time required for convergence can be divided by N_{atom}. Note that the MD runs can be performed in parallel, even with the same initial structures, as the initial velocities are randomly assigned.

With the calculated D at the four temperatures, the activation energy E_{a} can be obtained by fitting the Arrhenius relation, as shown in Fig. 4(a), where the D values (filled squares) are derived from the averages over the 500 MD runs. The four selected temperatures yield equally spaced points along the horizontal axis ($1000/T$). To illustrate the distribution of the data when fewer MD runs are used to obtain D, figure 4(a) also shows the D values obtained by 50 MD runs. Thus, at each temperature there are 10 data points (empty squares), which actually exhibit non-negligible deviations from the mean values. Figure 4(b) shows the convergence of E_{a} with respect to n (the number of MD runs). It is seen that when n is greater than 200 runs, the calculated E_{a} converges to about 0.01 eV.

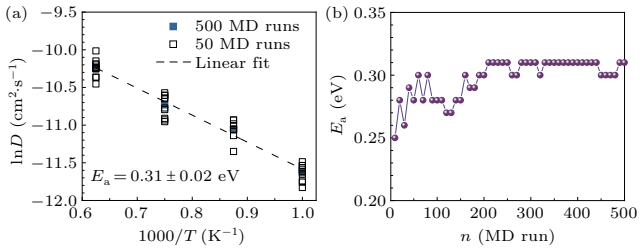


Fig. 4. (a) Arrhenius plot of the diffusion coefficient D and temperature T. The data points with filled squares were obtained by averaging over 500 60-ps MD runs, while the data points with empty squares were obtained by averaging over 50 60-ps MD runs through dividing the 500 runs into 10 sets. (b) Convergence of derived E_{a} as a function of n, the number of MD runs.

The converged E_{a} from the MD method is 0.31 eV with a fitting error of ±0.02 eV. This aligns with the diffusion barrier determined using the NEB method (0.31 eV), providing support for the reliability of the MD method for calculating the activation energy. By extrapolating the Arrhenius relation to room temperature, the diffusion coefficient D is calculated to be 2.2×10^{-9} cm^2·s^{-1}, which is on the same order of magnitude as that evaluated using the NEB method (4.3×10^{-9} cm^2·s^{-1}), reinforcing the consistency of the two methods.

4. Conclusion

We carried out a comparative study on the two commonly used methods, namely, NEB and MD, for studying the diffusion kinetics in solid-state electrolytes. We chose Na interstitial diffusion in MgO as the benchmark, which exhibits a well-defined diffusion path so that the two methods can yield directly comparable results. Using the NEB method, we calculated the diffusion barrier (E_b) to be 0.31 eV, from which the estimated diffusion coefficient D at room temperature is 4.3×10^{-9} cm^2·s^{-1}. Using the MD method, we acquired the D values at four high temperatures from 1000 K to 1600 K, from which the extracted activation barrier (E_a) is 0.31 ± 0.02 eV. The diffusion coefficient D of 2.2×10^{-9} cm^2·s^{-1} at room temperature was obtained by extrapolation. The consistent results between the two methods justify the reliability of the MD method, which currently relies on simulations at high temperatures and extrapolation to room temperature. Even though this benchmark is based on a single-path diffusion, we expect similar reliability of the MD method for multiple-path diffusion, for which the applicability of the NEB method becomes limited. In addition, we carefully studied the convergence issue of the MD method and found that the total effective simulation time of about 12 ns is required to achieve an accuracy of 0.01 eV for the activation energy in typical solid-state electrolytes.

Acknowledgments

Project supported by the National Natural Science Foundation of China (Grant Nos. 12164019, 11991060, 12088101, and U1930402) and the Natural Science Foundation of Jiangxi Province of China (Grant No. 20212BAB201017).

References

[1] Zhao Y, *et al.* 2023 *Nat. Rev. Mater.* **8** 623
[2] Yang C, *et al.* 2021 *Adv. Energy Mater.* **11** 2000974
[3] Tarascon J M and Armand M 2001 *Nature* **414** 359
[4] Chao D, *et al.* 2020 *Sci. Adv.* **6** eaba4098
[5] Wu F, Maier J and Yu Y 2020 *Chem. Soc. Rev.* **49** 1569
[6] Zhang Z, *et al.* 2018 *Energy Environ. Sci.* **11** 1945
[7] Janek J and Zeier W G 2016 *Nat. Energy* **1** 16141
[8] Zhu Z, *et al.* 2021 *Adv. Energy Mater.* **11** 2003196
[9] Oh K and Kang K 2020 *Angew. Chem. Int. Ed.* **59** 18457
[10] Zhang Z, *et al.* 2019 *J. Am. Chem. Soc.* **141** 19360
[11] Gupta M K, *et al.* 2021 *Energy Environ. Sci.* **14** 6554
[12] Poletayev A D, *et al.* 2022 *Nat. Mater.* **21** 1066
[13] Zhang Z and Nazar L F 2022 *Nat. Rev. Mater.* **7** 389
[14] He X, Zhu Y and Mo Y 2017 *Nat. Commun.* **8** 15893
[15] Heo T W, *et al.* 2021 *npj Comput. Mater.* **7** 214
[16] Baktash A, *et al.* 2020 *npj Comput. Mater.* **6** 162
[17] Strauss F, *et al.* 2021 *Sci. Rep.* **11** 14073
[18] Golov A and Carrasco J 2022 *npj Comput. Mater.* **8** 187
[19] Wang Z and Shao G 2017 *J. Mater. Chem. A* **5** 21846
[20] Winter G and Gómez-Bombarelli R 2023 *J. Phys.: Energy* **5** 024004
[21] Mishin Y 2005 *Diffusion Processes in Advanced Technological Materials*, edited by Gupta D (Springer Berlin Heidelberg, Berlin, Heidelberg, 2005), pp. 113
[22] Voter A F and Doll J D 1984 *J. Chem. Phys.* **80** 5832
[23] Rong Z, *et al.* 2016 *J. Chem. Phys.* **145** 074112
[24] Henkelman G and Jósson H 2000 *J. Chem. Phys.* **113** 9978
[25] Yang J H, *et al.* 2015 *Phys. Rev. B* **91** 075202
[26] Wang Y, *et al.* 2014 *Chem. Mater.* **26** 5613
[27] Jalem R, *et al.* 2013 *Chem. Mater.* **25** 425
[28] de Klerk N J J, van der Maas E and Wagemaker M 2018 *ACS Appl. Energy Mater.* **1** 3230
[29] Wang Y, *et al.* 2015 *Nat. Mater.* **14** 1026
[30] Varley J B, *et al.* 2016 *ACS Energy Lett.* **2** 250
[31] Deng Z, *et al.* 2016 *Chem. Mater.* **29** 281
[32] Chang D, *et al.* 2018 *Chem. Mater.* **30** 8764
[33] He X, *et al.* 2018 *npj Comput. Mater.* **4** 18
[34] Xu Z, *et al.* 2023 *npj Comput. Mater.* **9** 105
[35] Kresse G and Furthmuller J 1996 *Phys. Rev. B* **54** 11169
[36] Kresse G and Joubert D 1999 *Phys. Rev. B* **59** 1758
[37] Perdew J P, Burke K and Ernzerhof M 1996 *Phys. Rev. Lett.* **77** 3865
[38] Mehrer H 2007 *Diffusion in solids: fundamentals, methods, materials, diffusion-controlled processes* (Springer Science & Business Media, 2007), Vol. 155
[39] Wert C and Zener C 1949 *Phys. Rev.* **76** 1169
[40] Vineyard G H 1957 *J. Phys. Chem. Solids* **3** 121
[41] Nosé S 2006 *Mol. Phys.* **52** 255
[42] Wu X, *et al.* 2022 *Phys. Rev. B* **105** 195206
[43] Jinnouchi R, *et al.* 2019 *Phys. Rev. Lett.* **122** 225701
[44] Jinnouchi R, *et al.* 2020 *J. Chem. Phys.* **152** 234102
[45] Jinnouchi R, Karsai F and Kresse G 2019 *Phys. Rev. B* **100** 014105
[46] Shi J, *et al.* 2023 *J. Mater. Chem. A* **11** 14819
[47] Smith D K and Leider H R 1968 *J. Appl. Crystallogr.* **1** 246